Study of a Fabry–Perot Cavity in the Microwave Frequency Range by the Boundary Element Method

Hervé Cam, Serge Toutain, *Member, IEEE,* Philippe Gelin, *Member, IEEE,* and Gabrielle Landrac

Abstract—**In order to describe very closely the operation of a quasi-optical multidiode oscillator using a Fabry–Perot cavity, each component must be modeled. This paper presents the description of such a cavity by the Boundary Element Method (BEM).**

The difficulties of adapting classical models to this practical case are discussed in the first part of the paper and justify the use of a more complete and flexible method such as the three dimensional Boundary Element Method. Two levels of approach are succinctly described in the second part. The first one, which has been called zero order, is quite classical. The second one is the most original part of the study and has been called the Second Order Approach. The evolution of the computed results as a function of the number and the distribution of the meshes is given in the last part. They are compared to analytical results and measurements.

I. Introduction

SINCE THE emergence of solid state microwave sources, many studies have been made to improve their performance. Nowadays, in the millimetric frequency range, such solid state oscillators are a good alternative in cases where low power capabilities are required. In order to obtain higher power levels, the concept of multidiode oscillators was introduced in 1970 by Kurokawa [1]. Since then, several solutions have been proposed, but generally these solutions are not usable in the millimetric wavelength range because of mechanical problems.

The design of power adders using quasi-optical resonators does not seem to be limited by such problems [2], [3]. However the mastering of all the design problems requires great accuracy in the determination of the electromagnetic characteristic of the device. In relation with the general problem of power adding in the millimetric wavelength range, this paper deals with the modeling of a Fabry–Perot resonator by the Boundary Element Method (BEM).

In the first part, we discuss the classical approach of quasi-optical cavities and present the limitations to their application in the case under study. In the second part, the basis of the BEM is recalled and its application to the Fabry–Perot resonator is presented. Two levels of approach, corresponding to different levels of approximation are presented: the second one is the improvement to the method that we propose. In the last part of the paper, theoretical results are compared to experimental data.

Manuscript received June 21, 1990; revised August 27, 1991.

The authors are with the Laboratoire d'Electronique et Système de Télécommunications URA CNRS-1329, Ecole Nationale Supérieure des Télécommunications de Bretagne, BP 832, 29285 Brest Cedex, France.

IEEE Log Number 9104782.

II. Modeling of the Quasi-Optical Cavity: the Classical Approach

The model which is classically used to describe the Fabry–Perot cavity was mainly developed in the sixties for MASER cavities characterization. Assuming certain hypotheses, analytical formulation enables the main characteristics to be determined: that is to say, the resonance frequencies, and the field pattern of each mode. The simplifying hypotheses suppose that the solutions are similar to those of plane waves, and lead to different formulations according to the way that the problem is treated.

For the formulation proposed by A. G. Fox and T. Li [4] the evolution of the electromagnetic fields is followed during a "there and back journey" into the cavity. Starting from one reflector, the electromagnetic fields successively undergo a diffraction, from the first reflector to the second one, then a reflection off the second reflector, a diffraction towards the first reflector, to be finally reflected of it. If the phases are identical before and after the journey, the cavity resonates. The previous simplifying hypotheses, applied to this formulation, lead to the Huygens–Fresnel hypothesis [5]: the diffraction angles are very small.

Another way to formulate the problem is to solve the Helmholtz equation [6] directly. The simplifying hypothesis now expresses that the propagating constant of each mode is $2\pi/\lambda$, where λ is the wavelength at the resonat frequency. These two formulations give the same results.

A generalization of these formulations has been given by G. Goubau and F. Schwering [7] to take into account the diffraction losses on the reflectors; the solution is expressed as a series of cylindrical waves.

In order to characterize modes, it is possible to represent these by their current distribution in the mirrors. Some examples of two types of modes are presented in Fig. 1. Two kinds of representations of the current distribution are given in the paper: with arrows which gives the module and the direction of current lines over the mirrors

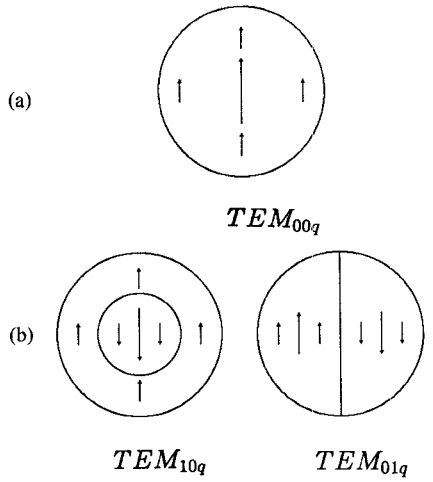

Fig. 1. Current distribution for (a) a Guassian mode and (b) for two loss modes.

and a meshed representation which only gives the module of the currents.

In the case of low-loss modes, the use of the analytical model leads to very good results for determining the characteristics of the resonant modes of the cavity. To be able to optimize the operation of the power adder using a quasi-optical cavity, the entire device must be modeled. In such a device the cavity is no longer isolated but is coupled to sources and to a load by coupling elements which will disturb the operation of the cavity. Classical models are not very easy to adapt to this practical case, because they do not have the flexibility of numerical methods, especially when the latter describe the structures by a meshing. We have chosen to apply the BEM to this problem and we present the results obtained with a Fabry–Perot cavity. The aim of this paper is not only to give a new description of this kind of cavity, but to demonstrate the applicability of this numerical method to such a structure. Reliability is verified by a comparison with the analytical approach and with experimental results.

II. Description of the Method

A. General Points

Today, numerical methods are widely used to solve physical problems in various areas such as elastostatics or electromagnetism. The Finite-Element Method is certainly the most well-known of all: it allows very complicated structures to be described with very great accuracy. However, it often requires a very large computer memory to solve the final matrix equation: the structure must be described in its entirely.

The BEM was proposed in the 80's [8] in order to represent a structure through its discontinuities: only the boundary conditions are written. Thus the problem can be treated with one dimension loss by the BEM than by the Finite-Element Method. The discontinuities are treated by the BEM as radiating apertures: the superposition of the fields radiated by the discontinuities, allows the fields to be determined everywhere on the structure, and in particular on the discontinuities themselves, when a set of integral equations is required. For example, when discontinuities are infinitely conductive metallic planes, we have

$$\begin{cases} \vec{n} \times \vec{E} = \vec{0} \\ \vec{n} \cdot \vec{H} = 0 \end{cases} \tag{1}$$

The radiated fields $\vec{E}$ and $\vec{H}$ are expressed in terms of fictitious sources, through the Green functions [9]:

$$\begin{cases} \vec{E}(r') = \dfrac{1}{4\pi} \displaystyle\iint_S [-j\omega\mu(\vec{n} \times \vec{H})\Psi + (\vec{n} \times \vec{E}) \times \vec{\nabla}\Psi \\ \qquad + \dfrac{1}{j\omega\epsilon} (\vec{n} \times \vec{H}) \cdot \vec{\nabla}(\vec{\nabla}\Psi)]\, dS \\ \vec{H}(r') = \dfrac{1}{4\pi} \displaystyle\iint_S [j\omega\epsilon(\vec{n} \times \vec{E})\Psi + (\vec{n} \times \vec{H}) \times \vec{\nabla}\Psi \\ \qquad - \dfrac{1}{j\omega\mu} (\vec{n} \times \vec{E}) \cdot \vec{\nabla}(\vec{\nabla}\Psi)]\, dS. \end{cases} \tag{2}$$

$\vec{E}(r')$ and $\vec{H}(r')$ are the electric and magnetic fields, radiated by the aperture of surface S.

$\vec{n}$ is the normal vector to dS.

Ψ is the Green function: $\Psi = \exp(-jkR)/R$ in the three dimensional case.

If no external field is applied, the boundary conditions (1) applied to (2) gives

$$\frac{1}{2}\vec{H}(r') = \frac{1}{4\pi} \iint_S (\vec{n}(r) \times \vec{H}(r)) \times \vec{\nabla}\Psi(r, r')\, dS \tag{3}$$

and assuming $\vec{J} = \vec{n} \times \vec{H}$, to be the electric current on the discontinuities, (3) becomes

$$\frac{1}{2}\vec{J}(r') = \frac{1}{4\pi} \vec{n}(r') \times \iint_S \vec{J}(r) \times \vec{\nabla}\Psi(r, r')\, dS. \tag{4}$$

The currents through the metallic parts of the resonator are described by (4). If $\vec{J} \neq \vec{0}$ the latter expresses the existence of a resonant mode.

The aim of the BEM is to solve such an equation.

B. Discretization of the Structure

The first step consists of discretizing the structure on a meshing, and projecting the (4) onto it. Equation (4) can then be transformed into

$$\frac{1}{2}\vec{J}^i(r') = \frac{1}{4\pi} \sum_{j=1}^{N} \iint_{Sj} \vec{n}^i \times (\vec{J}^j(r) \times \vec{\nabla}\Psi(r, r'))\, dS \tag{5}$$

where N represents the number of meshes. And using

$$\begin{cases} \vec{J}^i = J_x^i \vec{i} + J_y^i \vec{j} + J_z^i \vec{k} \\ \vec{n}^j = n_x^j \vec{i} + n_y^j \vec{j} + n_z^j \vec{k} \\ \vec{\nabla}\Psi = \dfrac{\partial\Psi}{\partial x} \vec{i} + \dfrac{\partial\Psi}{\partial y} \vec{j} + \dfrac{\partial\Psi}{\partial z} \vec{k} \end{cases} \tag{6}$$

(5) becomes

$$\left[\begin{aligned}
\frac{1}{2}J_x^i &= \sum_{j=1}^{N}\left(\iint_{S^j} J_x^j A_{1,1}^{i,j}\,d\Gamma + \iint_{S^j} J_y^i A_{1,2}^{i,j}\,d\Gamma \right.\\
&\qquad \left. + \iint_{S^j} J_z^j A_{1,3}^{i,j}\,d\Gamma\right)\\
\frac{1}{2}J_y^i &= \sum_{j=1}^{N}\left(\iint_{S^j} J_x^j A_{2,1}^{i,j}\,d\Gamma + \iint_{S^j} J_y^j A_{2,2}^{i,j}\,d\Gamma \right.\\
&\qquad \left. + \iint_{S^j} J_z^j A_{2,3}^{i,j}\,d\Gamma\right)\\
\frac{1}{2}J_z^i &= \sum_{j=1}^{N}\left(\iint_{S^j} J_x^j A_{3,1}^{i,j}\,d\Gamma + \iint_{S^j} J_y^j A_{3,2}^{i,j}\,d\Gamma \right.\\
&\qquad \left. + \iint_{S^j} J_z^j A_{3,3}^{i,j}\,d\Gamma\right)
\end{aligned}\right. \tag{7}$$

In the previous system the index "i" refers to the point where the current is calculated, and the index "j" to the sources of the fields. The calculated currents are linked field sources by $A_{\alpha,\beta}^{i,j}$ (with $(\alpha, \beta) = 1 \cdots 3$), whose values are listed as follows:

$$\left\{\begin{aligned}
A_{1,1}^{i,j} &= \vec{n}^i \vec{\nabla}\Psi(ri, rj) - n_x^i \frac{\partial \Psi}{\partial x}(ri, rj)\\
A_{1,2}^{i,j} &= -n_y^i \frac{\partial \Psi}{\partial x}(ri, rj)\\
A_{1,3}^{i,j} &= -n_z^i \frac{\partial \Psi}{\partial x}(ri, rj)
\end{aligned}\right. \tag{8}$$

$$\left\{\begin{aligned}
A_{2,1}^{i,j} &= -n_x^i \frac{\partial \Psi}{\partial y}(ri, rj)
\end{aligned}\right. \tag{9}$$

$$\left\{\begin{aligned}
A_{2,2}^{i,j} &= \vec{n}^i \vec{\nabla}\Psi(ri, rj) - n_y^i \frac{\partial \Psi}{\partial y}(ri, rj)\\
A_{2,3}^{i,j} &= -n_z^i \frac{\partial \Psi}{\partial y}(ri, rj)
\end{aligned}\right. \tag{10}$$

$$\left\{\begin{aligned}
A_{3,1}^{i,j} &= -n_x^i \frac{\partial \Psi}{\partial z}(ri, rj)
\end{aligned}\right. \tag{11}$$

$$\left\{\begin{aligned}
A_{3,2}^{i,j} &= -n_y^i \frac{\partial \Psi}{\partial z}(ri, rj)
\end{aligned}\right. \tag{12}$$

$$\left\{\begin{aligned}
A_{3,3}^{i,j} &= \vec{n}^i \vec{\nabla}\Psi(ri, rj) - n_z^i \frac{\partial \Psi}{\partial z}(ri, rj).
\end{aligned}\right.$$

C. Transformation of the Integral System Into a Linear System

System (7) is an eigen integral system, with "$1 + j0$" as the eigenvalue. Such a system, with this form, is not easily computable. This step is intended to transform the latter into a linear system, assuming some simplifying hypotheses on $\vec{J}$.

Two simplifying levels can be considered:

The zero order approach is very close to the description presented by W. Geyi and W. Hongshi [10]. They have applied this description to rectangular, cylindrical and spherical cavity resonators.

The second order approach, which is the most original part of the study, enables the accuracy of the results obtained to be improved. In this way the description is more realistic and more complete than the former.

D. The Zero Order Approach

For a zero order approach, the electric current $\vec{J}$ is assumed to be constant on the mesh. This allows J_x^i, J_y^i and J_z^i to be extracted from the integrals of the previous system. Thus, the latter can be expressed as

$$\frac{1}{2}\begin{pmatrix} J_x \\ J_y \\ J_z \end{pmatrix} = \begin{pmatrix} B_{1,1} & B_{1,2} & B_{1,3} \\ B_{2,1} & B_{2,2} & B_{2,3} \\ B_{3,1} & B_{3,2} & B_{3,3} \end{pmatrix}\begin{pmatrix} J_x \\ J_y \\ J_z \end{pmatrix}. \tag{13}$$

In this equation, the $B_{i,j}(i, j = 1 \cdots 3)$ are complex, and only depend on $k = k' + jk''$, the propagation constant throughout the Green function Ψ: this is the unknown factor of the problem.

E. The Second Order Approach

In order to describe a discontinuity with a zero order approach, many meshes are often required to achieve preciseness. This is the case, for instance, when the discontinuities to be described are not plane, or when the currents remain confined in particular areas of the surface. Under these conditions, the matricial systems to solve can rapidly reach prohibitive sizes.

For a second order approach, six points of a triangular mesh and eight points of a rectangular mesh supply functions for a quadratic interpolation of the coordinates and the currents on the mesh. The nodes are located on the vertices and on each side of the mesh.

A second order approach, unlike the zero order approach, enables non plane meshes to be described. In the same way as above, it is possible to achieve a matricial system, similar to (13).

F. Determination of the Resonant Mode

The problem consists of finding k_0 for which system (13) has a non-trivial solution. This is verified when

$$f(k = k_0) = \det\begin{bmatrix} B_{1,1} - Id & B_{1,2} & B_{1,3} \\ B_{2,1} & B_{2,2} - Id & B_{2,3} \\ B_{3,1} & B_{3,2} & B_{3,3} - Id \end{bmatrix} = 0. \tag{14}$$

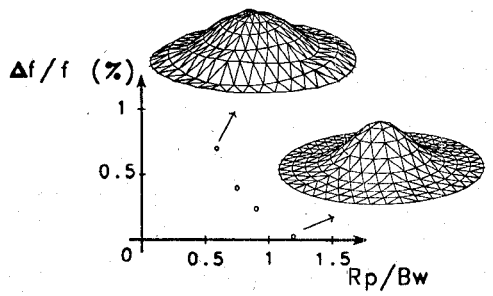

Fig. 2. Evolution of the resonant frequency as a function of the ratio plane mirror radius over beam waist.

Condition (14) gives k_0, which enables the frequency of the resonant mode to be calculated, as well as its quality factor (15):

$$k_0 = k_0' + jk_0'' \rightarrow \begin{cases} f = k_0' C/2\pi \\ Q = k_0'/k_0'' \end{cases}. \tag{15}$$

Then the problem consists in finding the value of k_0 which cancels the determinant in the complex plane. For the present work, the Muller method was used [11].

When k_0 is determined, the eigenvector $\vec{J}$ can then be computed. The great dimensions of the matrix B prevent the use of conventional methods such as Gaussian method. A second order iterative process gives very good results for this case [12].

At this step in the study, the interest of using the BEM appears first in relation to the geometrical parameters of the cavity. So, to illustrate the possible of the BEM, we compared the calculated frequencies obtained by the BEM when the radius of the plane mirror varies, to the frequency calculated by the analytical formulation. As the results obtained are identical when the radius of the plane mirror is great (i.e., when the losses are low), they diverge when it decreases. Fig. 2 shows the evolution of the resonant frequency of a Gaussian mode (TEM_{00q}) as a function of the plane mirror radius. In this figure R_p represents the radius of the plane mirror and B_w the beam waist. This latter is a parameter of the beam in the classical description: it represents the beam radius at $1/e$ of the maximum amplitude of the field. It is important to notice that when the diffraction losses increase, the mode is no longer a purely Gaussian mode but a superposition of modes where the TEM_{00q} still remains dominant. From this point of view, these results can be compared to the formulation by Goubau and Schwering [7].

In the analytical formulations, the characteristics of the solution depend on the symmetry of the problem: if the mirrors are circular the solutions are of cylindrical type. The computations that we have performed have shown that modes with a Cartesian symmetry can be excited too: Figure 3 gives one example of such a mode.

The last illustration, which is presented in this paper, concerns the disturbances on a TEM_{00q} mode, brought by an iris placed in the center of the plane mirror of the cavity. It is to be noticed that this mode can continue to exist, only if the perturbances are weak. The simulation results

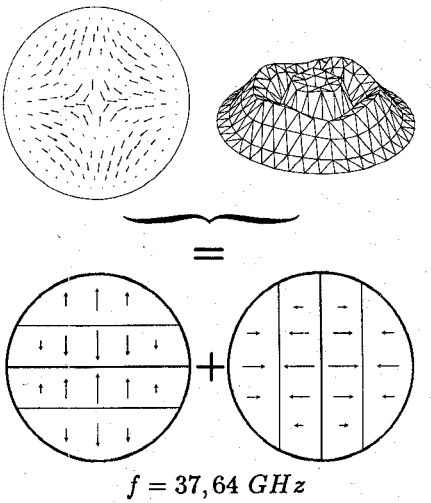

Fig. 3. Examples of modes with a Cartesian symmetry excited in a structure with a cylindrical symmetry.

presented in Fig. 4, show the surface currents computed on the plane mirror. The iris radius is 0.1 λ_0 where λ_0 is the wavelength at the resonant frequency. The computations have shown no variation of the frequency of the TEM_{00q} mode, linked to the disturbance brought by the iris.

It is to be noticed that the Three Dimensional Boundary Element Method can be very time consuming. The Muller method is very reliable in the sense that it almost never diverges, but its convergence speed is very low: it often requires more than 20 iterations to reach the result.

IV. Characterization of a Fabry-Perot Cavity by the BEM

A. General Points

The identification of the modes computed by the BEM with the results given by the analytical models is only possible by an examination of the fields of the resonant mode. For certain modes, identification poses problems because it is impossible to identify them clearly to TEM_{plq} modes. So the question is to know if these modes are really excitable in a cavity or if they are only spurious modes, linked with the method. This is the reason why the computations have been compared to measurements.

The previous method has been applied to a quasi-optical cavity, using a spherical mirror facing a flat mirror. The spherical mirror is placed on a special mounting, which ensures that the mirrors are aligned. The adjusting of the distance between the mirrors is made by micrometric displacements. The characteristics of the cavity are

$$\begin{cases} \text{Curvature radius of the spherical mirror: 40 mm} \\ \text{Diameter of the spherical mirror: 70 mm} \\ \text{Diameter of the plane mirror: 37 mm} \\ \text{Mirror separation: 29.1 mm} \end{cases} \tag{16}$$

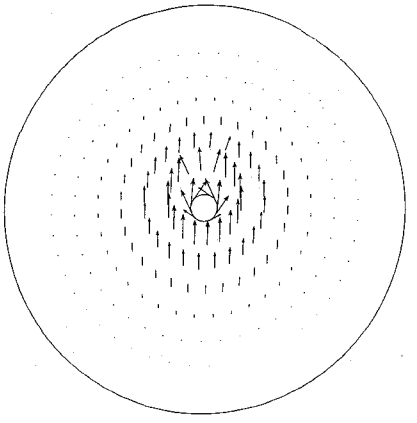

Fig. 4. Current distribution on the plane mirror of a cavity disturbed by an iris.

TABLE I

BEM: 96 Meshes				
Zero Order	Second Order	Analytical Method	Experimental Results	
—	f = 39.4 GHz	—	f = 39.3 GHz	
—	Q = 400	—		
f = 38.33 GHz	f = 37.77 GHz	f = 37.78 GHz	f = 37.7 GHz	TEM_{007}
Q = 492	Q = 1193			
f = 36.6 GHz	f = 36.0 GHz	—	f = 35.9 GHz	
Q = 245	Q = 1465	—		

The characteristics of the cavity are measured by a reflectometric method. The cavity is excited by a hole, located just in the center of the plane mirror. It is a setup which naturally favours the modes with energy around the axis of the cavity. All the results which are presented in the continuation concern modes whose energy is maximum on the axis of the cavity: this enables the excited modes to be identified. The reliability of the measurements of the resonant frequency is, for the main part, linked with the accuracy of measurements of the distance separating the mirrors. It can be evaluated to 5×10^{-2} mm, which leads to an inaccuracy of about 70 MHz in the measurements.

B. Comparison Between Experimental Results and Models

The results obtained by the zero and second order approaches, are compared to those obtained by the analytical methods (when it is possible), and to experiments. We recall the equation which gives the value of the resonant frequencies of such a structure:

$$f_{p,l,q} = \frac{C}{2D}\left\{q + \frac{(2p + l + 1)}{\pi} \arctan\left[\left(\frac{D}{R_0 - D}\right)^{1/2}\right]\right\} \tag{17}$$

where

Indices p and l are the radial and transversal indices respectively: they are the beam parameters.

Indice q determines the number of half wavelengths between the two resonators.

D is the distance between the reflectors and R_0 the curvature radius of the spherical mirror.

Table I is given for a constant number of meshes.

Fig. 5 summarizes the measurements undertaken on the cavity and the fields obtained by the BEM modeling in the 35 GHz–40 GHz range.

As a result of this, several remarks can be made:

It is possible to compare analytical results to numerical results only when the mode can be perfectly identified. This can be done by examining the fields of the resonant mode. This was only possible for the TEM_{007} mode.

The zero order approach gives results whose frequencies are systematically lower than the frequencies measured and lower than second order results by a factor $\Delta f/f_0$ of about 1%. For such an approach the meshes are plane and the origin of the coordinates of $\vec{J}$ is taken at the center of the mesh. This provokes a relative reduction in the distance between the mirrors, which is about $\Delta f/f_0$. This is certainly the main reason for the inaccuracy of that approach, when it is applied to our structure. However, because of the simplicity of its implementation, it is of interest to use it first to characterize complicated structures.

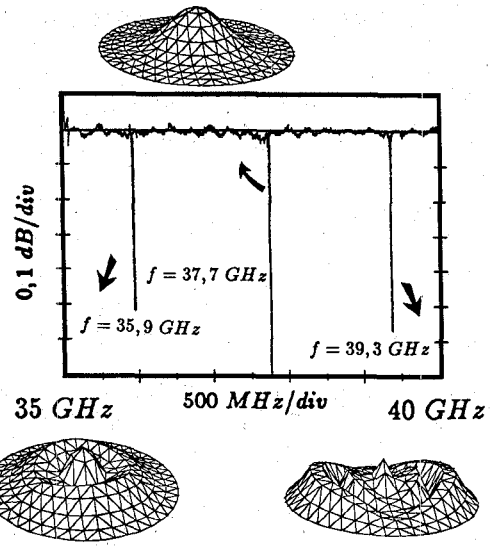

Fig. 5. Response of the cavity between 35 GHz and 40 GHz: comparison between measurement and the BEM modeling.

TABLE II
TEM_{007} MODE

BEM	Second Order Approach		
	61 Nodes	127 Nodes	217 Nodes
Uniform meshing	f = 37.84 GHz Q = 337	f = 37.80 GHz Q = 886	f = 37.77 GHz Q = 1193
Meshing nonuniformly concentrated	f = 37.80 GHz Q = 1931	f = 37.76 GHz Q = 1707	f = 37.74 GHz Q = 8201
Analytical method	f = 37.78 GHz		

Results obtained by the second order approach are very close to experimental results.

The quality coefficient compared gives a good indication about the reliability of the calculations. It is to be noted that the second order approach gives more reliable results.

The accuracy of the results depends on the preciseness of the description of the structure. It is foreseeable that reliability will increase with the number of meshes. Another possibility consists of refining the description of the structure where the surface currents are the highest. Table II gives the evolution of the results for a second order approach for the TEM_{007} mode, when the number of meshes varies and when the meshes are concentrated on the center of the mirrors.

The results presented show great accuracy, even when the number of meshes is low. The size of the matrix to be processed increases as the square of the number of nodes and the computing times for each iteration increase faster than its cube. So the number of meshes to use must be a compromise between the preciseness to be achieved and the computing times. The second remark that can be made, concerns the influence of the concentration of the meshes on the discontinuities: the results clearly show the advantage in concentrating the number of meshes in the areas where the currents are the greatest.

V. Conclusion

The results presented in this paper clearly show that the BEM is a very efficient method to characterize an open cavity, especially when a second order approach is used.

For the Gaussian mode (TEM_{00q}), the results obtained with the classical method are in close agreement with the computed results and with measurements. However they diverge when the spill-over losses of the cavity increase.

On the other hand, it is not possible to predict certain types of modes with the classical formulation: for the power combiner application it is of interest to have very accurate knowledge about the behavior of the cavity around the low losses mode to be excited.

Finally, the main interest of this method, in addition to its accuracy, is its great flexibility. The BEM computes currents on a discretized structure. So coupling elements like the iris are very naturally described as belonging to the cavity: the numerical computations associated remain unchanged.

These reasons allow equivalent performances to those presented here to be envisaged, when the coupling elements will be taken into account.

Acknowledgment

We should like to thank the systems team at ENST de Bretagne for all the help they have given us, and IFREMER in Brest for letting us use their computing facilities.

References

[1] K. Chang and C. Sung, "Millimeter-wave power-combining techniques," *IEEE Trans. Microwave Theory Tech.*, vol. MTT-31, no. 2, pp. 91–107, Feb. 1983.
[2] L. Wandiger and V. Nalbandian, "Millimeter-wave power combiner using quasi optical techniques," *IEEE Trans. Microwave Theory Tech.*, vol. MTT-31, no. 2, pp. 189–193, Feb. 1983.
[3] S. L. Young and K. D. Stephan, "Stabilization and power combining of planar microwave oscillator with an open resonator," in *1987 IEEE MTT-S Int. Microwave Symp. Dig.*, Las Vegas, NV, June 1987, pp. 185–188.
[4] A. G. Fox and T. Li, "Resonant modes in a MASER interferometer," *Bell Syst. Tech. J.*, vol. 40, pp. 453–488, Mar. 1961.
[5] S. Silver, Ed., *Microwave Antenna Theory and Design*, IEE Electromagnetic Waves Series 19. London: Peregrinius, pp. 108–112, 1986.
[6] A. L. Cullen, "Millimeter-wave open-resonator techniques," *Infrared and Millimeter Wave*, vol. 10, Ch. 4, pp. 233–281, 1983.
[7] G. Goubau and F. Schwering, "On the guided propagation of electromagnetic wave beam," *IRE Trans. Antennas Propag.*, vol. AP-9, pp. 248–256, May 1961.
[8] C. A. Brebbia and S. Walker, *Boundary Element Technique in Engineering*. London: Newnes-Butterworths, 1980.
[9] J. A. Stratton, *Electromagnetic Theory*. New York: McGraw-Hill, pp. 464–468, 1941.
[10] W. Geyi and W. Hongshi, "Solution of the resonant frequencies of a cavity resonator by boundary element method (BEM)," IEE Proc., vol. 135, pt. H, no. 6, pp. 361–365, Dec. 1988.
[11] E. Durand, *Solutions Numériques des Equations Algébriques: Equations du Type—F(X) = 0—Racine d'un Polynôme*, vol. 1. Paris: Masson et Cie, pp. 270–273, 1971.
[12] E. Durand, *Solutions Numériques des Equations Algébriques: Système de Plusiers Equations—Valeurs Propres des Matrices*, vol. 2. Paris: Mason et Cie, pp. 368–379, 1972.

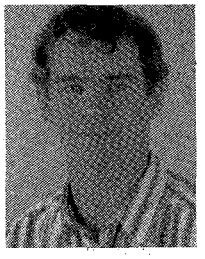

Hervé Cam was born in 1961 in Paris. In 1988 he graduated from "Ecole Nationale Supérieure des Télécommunications de Bretagne." He is presently a researcher pursuing the Ph.D degree in the Electronics and Physics Department of ENSTBr.

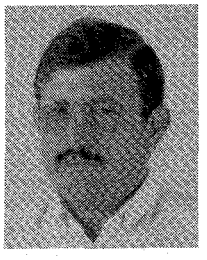

Serge Toutain (M'84) is presently Professor of Electrical Engineering at "Ecole Nationale Supérieure des Télécommunications de Bretagne" and head of the Electronics and Physics Department. He is interested in electromagnetic theory and the design of passive and active integrated millimeter circuits and technologies.

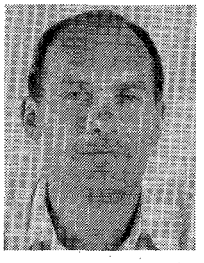

Philippe Gelin (M'91) is presently a Professor of Electrical Engineering at "Ecole Nationale Supérieure des Télécommunications de Bretagne." His research interests are in the area of electromagnetic theory, computing methods applied to the study of discontinuities, and propagation in ferrimagnetic media.

Gabrielle Landrac was born in 1964 in Brest, France. In 1986 she graduated from "Ecole Nationale Superieure des Télécommunications de Bretagne" and received a Ph.D. degree in electronics in 1989.

She is currently working at LEST-ENSTBr (Laboratoire d'Electronique et des systèmes de Télécommunications) as a Research Lecturer. Her research interests involve discontinuities in open waveguides and the interaction between discontinuities in relation with antennas and circuits at millimeter wavelengths.